Aerospace Science and Technology 82–83 (2018) 583–593

Contents lists available at ScienceDirect

Aerospace Science and Technology

www.elsevier.com/locate/aescte

Iterative learning control and initial value estimation for probe–drogue autonomous aerial refueling of UAVs

Xunhua Dai **, Quan Quan *, Jinrui Ren, Kai-Yuan Cai

School of Automation Science and Electrical Engineering, Beihang University, Beijing, 100191, China

ARTICLE INFO

Article history:
Received 8 June 2018
Received in revised form 16 August 2018
Accepted 26 September 2018
Available online 2 October 2018

Keywords:
Autonomous aerial refueling
Iterative learning control
Bow wave effect
Aerodynamic disturbances
UAV

ABSTRACT

In a probe–drogue aerial refueling system, the drogue is affected not only by wind disturbances but also by strong disturbances from the tanker vortex and receiver forebody bow wave. Along with the aerodynamic disturbances acting on the receiver aircraft, it is difficult for the probe to capture the moving drogue in the docking stage. This paper studies the model of the probe–drogue aerial refueling system under aerodynamic disturbances, and proposes docking control method based on iterative learning control to compensate for the docking errors caused by aerodynamic disturbances. For receiver aircraft with different maneuverability, three control strategies are proposed to achieve a trade-off between safety and control precision. Furthermore, a practical method is proposed to predict the initial value of the learning controllers, which can significantly improve the iterative learning speed of the proposed methods. Finally, simulations demonstrate that the proposed control methods are simple and efficient for the docking control of autonomous probe–drogue aerial refueling.

1. Introduction

The autonomous aerial refueling (AAR) techniques make new missions and capabilities possible for future unmanned aerial vehicles (UAVs) through extending the range and endurance [1,2]. There are many types of aerial refueling methods, among which the probe–drogue refueling (PDR) method is considered to be more flexible and compact than other refueling methods, and it can be applied to different aircraft, different refueling speeds, and multiple aircraft refueling tasks [3]. However, a serious drawback of PDR is that the drogue is completely passive and susceptible to aerodynamic disturbances [3,4], because of which the autonomous docking control for the PDR system is still a difficult problem.

Distinguished by whether the disturbance is affected by the movement (state) of the receiver aircraft, the disturbances in the PDR docking stage can be divided into two types: state-independent disturbances and state-dependent disturbances. The state-independent disturbances mainly include the tanker vortex, prevailing wind, wind gust, and atmospheric turbulence [5,6], under the effect of which the drogue will eventually oscillate around an equilibrium position unrelated to the receiver movement. The state-dependent disturbances are mainly referred to as the bow wave effect or the forebody effect [7,8], under the effect of which the drogue will be pushed away by the forebody flow field of the receiver (see Fig. 1(a)) as the receiver comes close. If the state-dependent disturbances are not considered, then the docking control problem can be described as a classic trajectory tracking problem, which can be well solved by tracking control methods including LQR [9,10], L1 adaptive control [11,12] and back-stepping control [13,14]. However, it was found in the flight tests of NASA Autonomous Airborne Refueling Demonstration (AARD) project [1] that the bow wave effect may significantly affect the drogue movement and cause the failure of the docking control, which is hard to solve with traditional control method. Then the U.S. military has been trying to minimize the bow wave effect by increasing the length of the probe (see Fig. 1(b)) or mounting the probe away from the nose (see Fig. 1(c)). However, these modifications cannot solve the bow wave effect problem essentially, and the vibration, fragility, and vulnerability of the long probe may bring some new safety problems. Therefore, it is meaningful to overcome the docking problem under disturbances from the point of view of control.

For probe–drogue autonomous aerial refueling of UAVs, there are two key technologies. The first one is target sensing and measurement and the other is docking control. The target sensing and measurement focus on detecting the drogue and measuring the relative position between the probe and the drogue, which is the base of docking control. Since target sensing and measurement can be well solved by vision localization methods [10,15] or vision/GPS-based methods [16,17], this paper focuses on studying

* First corresponding author.
** Corresponding author.
E-mail addresses: dai@buaa.edu.cn (X. Dai), qq_buaa@buaa.edu.cn (Q. Quan).

https://doi.org/10.1016/j.ast.2018.09.034
1270-9638/

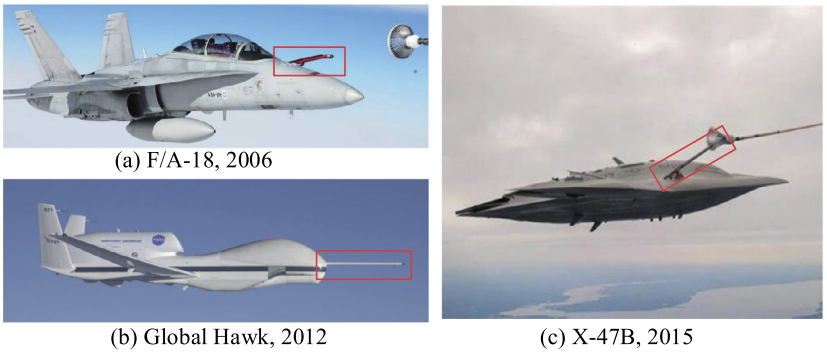

Fig. 1. Receiver aircraft of NASA AARD project.

the docking control for AAR systems. Considering that the drogue is much lighter than the receiver aircraft, when the drogue is pushed by the bow wave, the drogue may escape away with a speed much higher than that the receiver can capture. Meanwhile, chasing the drogue is also identified as a dangerous operation, which may cause the over control of the receiver [18]. Thus, as adopted by manned aerial refueling, the AAR control system needs to predict the final contact position of the drogue and the probe, and then drive the probe to the predicted position instead of chasing the moving drogue [19].

The iterative learning control (ILC) is a possible method to overcome the bow wave effect by learning from the previous repetitive docking attempts as human pilots do. According to the modeling research in [20,21], the bow wave effect model is highly nonlinear and complex, which is difficult to apply to controller design. Therefore, the ILC is more practical for AAR docking control because it does not require the exact mathematical model [22]. In our previous work [23], an ILC docking control method is proposed to overcome the bow wave effect of the PDR system by learning and predicting the final drogue position through repetitive docking attempts. The previously proposed control method is essentially a pure feedforward controller that the probe is always controlled to aim at a fixed position (the predicted drogue position) instead of tracking the drogue position, which is hard to handle the non-repetitive or random disturbances without tracking the drogue. In practice, for a receiver aircraft with high maneuverability flexible enough to catch up with the drogue movement, the introduction of feedback tracking control will help to decrease the docking error caused by non-repetitive disturbances. However, for heavy receiver aircraft with lower maneuverability and slower response speed, it is hard and unsafe to track the drogue directly due to the over control problem. Therefore, receiver aircraft with different maneuverability should adopt different control strategies for a trade-off between precision and safety.

Distinguished by whether the disturbance is predictable (repeatable) in different docking iterations, the disturbances can also be divided into repetitive disturbances and non-repetitive disturbances. The tanker vortex, the prevailing wind and the bow wave effect belong to repetitive disturbances because they will remain the same if the receiver moves along the same trajectory in each docking iteration; the wind gust and the atmospheric turbulence belong to non-repetitive disturbances because they are random or unknown in each docking iteration. Since ILC methods cannot completely compensate for the effect of the non-repetitive disturbances, measures should be proposed to minimize their effect or avoid dangerous docking attempt when the disturbances are too strong.

In this paper, motivated by the above facts, three control strategies based on ILC are proposed for receiver aircraft with different maneuverability, and the feedback tracking control is introduced into the ILC methods to improve the docking precision and success rate. Moreover, considering that the initial value is an important factor that affects the learning speed of ILC methods, this paper studies the PDR model and proposes an initial value estimation method to estimate the initial offset of the drogue position under different speeds and altitudes. The proposed initial value estimation method is also capable of making full use of the previous learning results under different refueling conditions. With the obtained initial value, the receiver can achieve a successful docking within about 2–3 learning attempts. Criteria are proposed to judge whether the flight condition (disturbance intensity) is suitable for a safe docking attempt. Since the relative distance between the drogue and the probe is usually measured by vision-based methods whose measurement precision depends on the relative distance (higher precision in a closer distance). Therefore, the proposed method is easy to apply to actual aerial refueling systems because it only needs the terminal positions (easy to measure with high precision) instead of the whole trajectories. Simulations based on our previously published MATLAB/SIMULINK environment [20,21] show that the proposed control method is simple, efficient and robust for an AAR system to overcome complex disturbances like the bow wave effect.

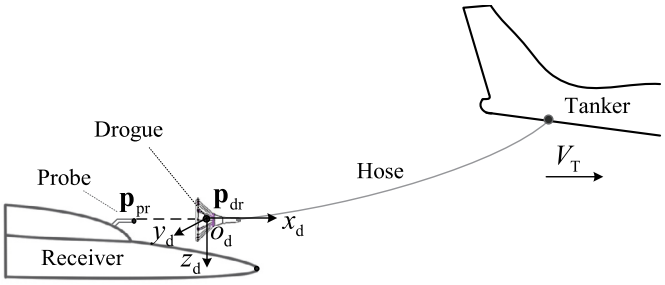

Fig. 2. Simplified schematic diagram of PDR systems.

The paper is organized as follows. Section 2 gives problem description and model analysis of PDR systems. Section 3 describes the ILC controller strategies with the convergence analysis, and then the initial value estimation method is proposed. Section 4 gives simulations and comparisons for the proposed ILC strategies, and the effect of the initial value estimation method is verified. Section 5 presents the conclusions and future work.

2. Problem formulation

2.1. Frames and notations

A typical PDR system is presented in Fig. 2, where the tanker makes a uniform linear motion with speed $V_T \in \mathbb{R}_+$, and the receiver control system controls the probe (on the receiver forebody) to dock into the drogue (at the end of the hose). Since the drogue will finally stabilize around an equilibrium point (relative

to the tanker body) without considering the state-dependent disturbances, a drogue frame $o_d x_d y_d z_d$ (see Fig. 2) is defined with the origin o_d located at that initial equilibrium position. Noteworthy, the origin o_d is fixed to the tanker instead of the drogue, so the drogue position $\mathbf{p}_{dr}$ will not be zero if it is pushed away from the initial equilibrium position.

For simplicity, the following rules are defined:

(i) All position or state vectors are defined under the drogue frame $o_d x_d y_d z_d$, unless explicitly stated.

(ii) The drogue position vector is expressed as $\mathbf{p}_{dr} \triangleq [x_{dr}\ y_{dr}\ z_{dr}]^T$, and the probe position vector is $\mathbf{p}_{pr} \triangleq [x_{pr}\ y_{pr}\ z_{pr}]^T$. In the same way, the position error between the probe and the drogue is expressed as

$$\Delta\mathbf{p}_{dr/pr}(t) \triangleq \mathbf{p}_{dr}(t) - \mathbf{p}_{pr}(t) \triangleq \begin{bmatrix} \Delta x_{dr/pr}(t) \\ \Delta y_{dr/pr}(t) \\ \Delta z_{dr/pr}(t) \end{bmatrix}. \tag{1}$$

(iii) According to the flight tests in the NASA report [1], the terminal time $T \in \mathbb{R}_+$ of a docking iteration should be defined as the first moment when the probe hit the drogue center plane ($\Delta x_{dr/pr} = 0$ as shown in Fig. 2), which is described in a mathematical form as

$$T = \arg\min_{t>0} \left(\Delta x_{dr/pr}(t) = 0\right) \tag{2}$$

(iv) The value at the terminal time $t = T$ is called the terminal value in this paper. For example, $\mathbf{p}_{dr}(T)$ denotes the terminal position of the drogue and $\Delta\mathbf{p}_{dr/pr}(T)$ denotes the terminal position error.

(v) The value in the kth docking iteration is marked by a right superscript. For example, $\mathbf{p}_{dr}^{(k)}(t)$ denotes the instantaneous drogue position $\mathbf{p}_{dr}(t)$ in the kth docking iteration, $T^{(k)}$ denotes the kth terminal time, and $\mathbf{p}_{dr}^{(k)}\left(T^{(k)}\right)$ denotes the terminal drogue position in the kth docking iteration.

2.2. Mathematical model

2.2.1. Hose–drogue model

The dynamics of the hose–drogue system can be modeled by a finite number of cylinder-shaped rigid links based on the finite-element theory [24,25], where the obtained hose–drogue dynamics is very complex with high nonlinearity and dimension. Since only the terminal position of the drogue $\mathbf{p}_{dr}^{(k)}\left(T^{(k)}\right)$ of each docking attempt is concerned for the convergence analysis of ILC method, this paper focuses on studying the model of the drogue terminal position.

Under the effect of nonrandom disturbances including wind gust and tanker vortex, the hose–drogue system will eventually stabilize at an equilibrium position. Then, the drogue position fluctuates around its equilibrium position under the effect of random disturbance (caused by the atmospheric turbulence) and bow wave effect. The random disturbance can be modeled by bounded colored noise [5], and the bow wave disturbance can be modeled by a decay function [21] related to the relative distance $\Delta\mathbf{p}_{dr/pr}$. Therefore, the terminal position of the drogue $\mathbf{p}_{dr}^{(k)}\left(T^{(k)}\right)$ can be described by

$$\mathbf{p}_{dr}^{(k)}\left(T^{(k)}\right) = \mathbf{w}_{dr}^{(k)} + \mathbf{f}_{bow}\left(\Delta\mathbf{p}_{dr/pr}^{(k)}\left(T^{(k)}\right)\right) \tag{3}$$

where $\mathbf{w}_{dr} \in \mathbb{R}^3$ represents the drogue position fluctuation caused by random disturbances with bound $\|\mathbf{w}_{dr}\| \le B_{dr}$, and $\mathbf{f}_{bow}(\cdot) \in \mathbb{R}^3$ represents the drogue position offset caused by the bow wave effect.

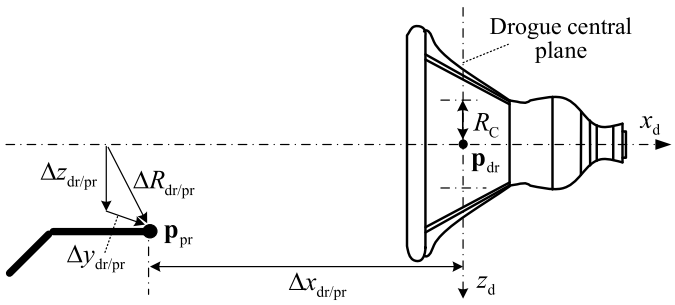

Fig. 3. Success and failure criteria of a docking attempt.

2.2.2. Receiver aircraft model

The receiver aircraft model includes the aircraft dynamics, the attitude and position control system, and aerodynamic disturbances. Similar to the analysis of the hose–drogue system, only the terminal position model of the receiver is considered here to simplify the problem. According to [6,26], when the autopilot system of an aircraft is well designed, the aircraft is capable of controlling the probe position $\mathbf{p}_{pr}$ to track the given reference trajectory $\hat{\mathbf{r}}_{pr} \in \mathbb{R}^3$. Therefore, when there is no disturbance during the docking stage, the probe can reach the desired position at the terminal time, namely, $\mathbf{p}_{pr^{(k)}}\left(T^{(k)}\right) = \hat{\mathbf{r}}_{pr}^{(k)}\left(T^{(k)}\right)$. However, in practice, there are many disturbances and other unpredictable factors that may affect the tracking effect at the terminal time T. Therefore, the actual position of the probe at each terminal time can be expressed as

$$\hat{\mathbf{r}}_{pr}^{(k)}\left(T^{(k)}\right) - \mathrm{p}_{pr}^{(k)}\left(T^{(k)}\right) = \mathbf{d}_{dr} + \mathbf{w}_{pr}^{(k)} \tag{4}$$

where $\mathbf{d}_{pr} \in \mathbb{R}^3$ is a constant disturbance term, and $\mathbf{w}_{pr} \in \mathbb{R}^3$ is a bounded random disturbance term with $\|\mathbf{w}_{pr}\| \le B_{pr}$. The constant disturbance $\mathbf{d}_{pr}$ may come from the response lag of the receiver or the repetitive disturbances such as the tanker vortex, the wind gust and the prevailing wind. The random disturbance $\mathbf{w}_{pr}$ may come from the non-repetitive disturbances such as atmospheric turbulence.

2.2.3. Objective of docking control

In each docking attempt (iterative process), the receiver stays a few meters behind the drogue for seconds until the hose–drogue system is stable. Then, the receiver starts to drive the probe to approach the drogue with a slow constant speed in x_d direction until the probe hits the central plane of the drogue as shown in Fig. 3. A radial error $\Delta R_{dr/pr} \in \mathbb{R}_+$ is defined for evaluating the docking performance as

$$\Delta R_{dr/pr}(t) \triangleq \sqrt{\Delta y_{dr/pr}^2(t) + \Delta z_{dr/pr}^2(t)}. \tag{5}$$

It is noteworthy that $\Delta R_{dr/pr}(T) \equiv \|\Delta\mathbf{p}_{dr/pr}(T)\|$ according to the definition $\Delta x_{dr/pr}(T) \equiv 0$ in Eq. (2). Since the docking error is inevitable due to disturbances, a threshold radius $R_C \in \mathbb{R}_+$ (referred to as the criterion radius in [1]) is defined as

$$\Delta R_{dr/pr}^{(k)}\left(T^{(k)}\right) < R_C. \tag{6}$$

If criterion (6) is satisfied at the kth docking attempt, a successful docking attempt is declared for this docking attempt. Otherwise, a failed docking attempt is declared.

3. ILC design

The role of the proposed ILC controller in an AAR system is the same as the human pilot in a manned aerial refueling system,

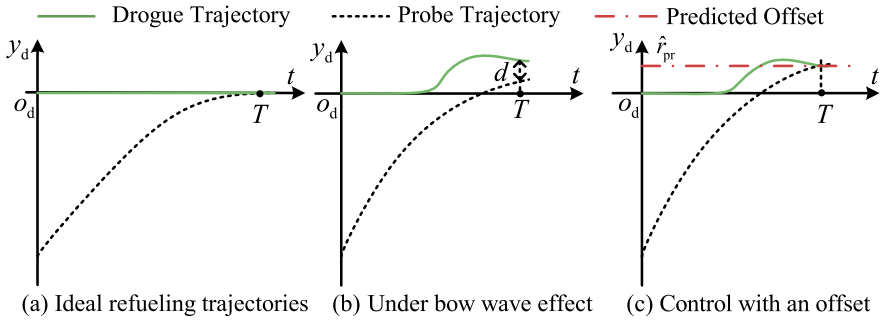

Fig. 4. Control problem under the bow wave effect.

which is more like an additional guidance module above the autopilot system. The inputs of the ILC controller are the historical trajectories of the probe and the drogue, and the output is the reference trajectory $\hat{\mathbf{r}}_{\mathrm{pr}}(t)$ which is further sent to the autopilot. This system structure can guarantee the minimum modification to the original control system, which is more simple and practical than the traditional ILC methods.

If there is no disturbance during the docking stage, the drogue stays relatively still at its equilibrium position (defined as the origin point of the drogue frame $o_{\mathrm{d}}x_{\mathrm{d}}y_{\mathrm{d}}z_{\mathrm{d}}$ in Fig. 2), and the docking control can be easily achieved by controlling the probe to track the drogue as shown in Fig. 4(a). However, in practice, the drogue will be pushed away by the receiver flow field, and it is hard for the receiver to catch the moving drogue as shown in Fig. 4(b). Therefore, as shown in Fig. 4(c), human pilots usually control the probe to track the drogue with a predicted offset to compensate for the docking error. The predicted offset comes from experiences of learning and training, which can be realized by ILC methods.

Considering that a heavier receiver aircraft has lower maneuverability and slower response speed, it is hard and unsafe to track the drogue directly. However, for a small receiver with high maneuverability, the response speed is fast enough to track the drogue to decrease the docking error caused by random disturbances. Therefore, receiver aircraft with different maneuverability should have different control strategies: more feedback tracking control should be adopted by a smaller receiver; more feedforward prediction should be adopted by a larger receiver aircraft. According to the above analysis, three control strategies are proposed for receiver aircraft with different maneuverability. Meanwhile, since too many docking attempts are unacceptable for an AAR system, a method to estimate the drogue offset caused by disturbances is proposed, which is effective to improve the learning speed of the proposed ILC methods.

3.1. Control Strategy 1

In order to compensate for docking errors through ILC, the simplest and safest control strategy is letting the probe always aim at a predicted fixed position during the docking stage. The predicted position $\hat{\mathbf{r}}_{\mathrm{pr}}^{(k)}$ for the autopilot is given by

$$\hat{\mathbf{r}}_{\mathrm{pr}}^{(k)}(t) = \mathbf{r}_{\mathrm{dr,bow}}^{(k)} \tag{7}$$

where $\mathbf{r}_{\mathrm{dr,bow}}^{(k)} \in \mathbb{R}^3$ is an estimation term for the drogue position offset which stays unchanged during each iteration. The update law for $\mathbf{r}_{\mathrm{dr,bow}}^{(k)}$ is given by

$$\mathbf{r}_{\mathrm{dr,bow}}^{(k)} = \mathbf{r}_{\mathrm{dr,bow}}^{(k-1)} + \mathbf{K}_p \cdot \Delta\mathbf{p}_{\mathrm{dr/pr}}^{(k-1)}\left(T^{(k-1)}\right), \tag{8}$$

where $\mathbf{K}_p = \mathrm{diag}\left(k_{p_1}, k_{p_2}, k_{p_3}\right)$ is a constant three-dimensional diagonal matrix with the diagonal elements $k_{p_1}, k_{p_2}, k_{p_3} \in (0, 1)$.

The following theorem provides the convergence condition under which one can conclude the convergence property of the designed ILC controller in Eq. (7).

Theorem 1. *Consider the AAR system with the terminal positions of the drogue and the probe satisfying Eq. (3) and Eq. (4) respectively. Suppose the ILC controller is designed as Eq. (7), and its parameters satisfy*

$$0 < k_{p_i} \leq 1, \quad i = 1, 2, 3. \tag{9}$$

Then, through the repetitive docking attempts, the docking error $\Delta\mathbf{p}_{\mathrm{dr/pr}}^{(k)}\left(T^{(k)}\right)$ *will converge to a bound*

$$\lim_{k\to\infty} \left\| \Delta\mathbf{p}_{\mathrm{dr/pr}}^{(k)}\left(T^{(k)}\right) \right\| \leq B_1 \tag{10}$$

where

$$B_1 = \frac{2\sqrt{B_{\mathrm{pr}}^2 + B_{\mathrm{dr}}^2}}{\min\limits_{i=1,2,3}\left\{k'_{p_i}\right\}} \tag{11}$$

in which B_{dr} *is the bound of the drogue position fluctuation as defined in Eq. (23) and* B_{pr} *is bound of the probe tracking error as defined in Eq. (4). In particular, if the random disturbances are negligible, i.e.,* $B_{\mathrm{dr}} = 0$, $B_{\mathrm{pr}} = 0$, *then the docking error will converge to zero, namely*

$$\left\| \Delta\mathbf{p}_{\mathrm{dr/pr}}^{(k)}\left(T^{(k)}\right) \right\| \to 0, \quad \text{as } k \to \infty. \tag{12}$$

Proof. See Appendix A. □

Under an ideal situation, for any specified threshold radius R_{C} as defined in Eq. (6), if the disturbances are small enough ($B_1 \to 0$), there is

$$\Delta R_{\mathrm{dr/pr}}^{(k)}\left(T^{(k)}\right) \leq B_1 \leq R_{\mathrm{C}}, \quad \text{as } k \to \infty$$

which means if the random disturbances are small enough, the docking attempt with *Control Strategy 1* will always succeed after enough docking attempts. However, in practice, B_1 is a little larger than R_{C}, and the docking attempts will succeed with a certain probability (the success rate). According to [1,19], if the aerodynamic disturbances are strong, both the position oscillation of the drogue and the tracking error of the receiver will be significant, then the success rate will be low. Therefore, if the convergence bound B_1 is large because of the severe weather condition or other factors, the AAR operation should be forbidden. In fact, a method to assess whether the conditions are suitable for the AAR is also an interesting research direction, which is very important and worth to be further investigated.

3.2. Control Strategy 2

Essentially, *Control Strategy 1* can be treated as a pure feedforward controller, which causes a significant decrease in the docking precision and success rate in the presence of random disturbances. In fact, for small UAVs with enough maneuverability to catch up with the drogue movement, the introduction of feedback control is quite necessary. Hence, another strategy is proposed as

$$\hat{\mathbf{r}}_{\mathrm{pr}}^{(k)}(t) = \mathbf{p}_{\mathrm{dr}}^{(k)}(t) + \mathbf{r}_{\mathrm{dr,off}}^{(k)} \tag{13}$$

where $\mathbf{p}_{\mathrm{dr}}^{(k)}(t)$ is the real-time drogue position in the kth docking attempt, and $\mathbf{r}_{\mathrm{dr,off}}^{(k)} \in \mathbb{R}^3$ is a constant iterative learning term. Unlike *Control Strategy 1*, $\hat{\mathbf{r}}_{\mathrm{pr}}^{(k)}(t)$ is not constant during each iteration and it will chase the drogue trajectory $\mathbf{p}_{\mathrm{dr}}^{(k)}(t)$, which means it contains a feedback control part to eliminate the tracking error. The update law for $\mathbf{r}_{\mathrm{dr,off}}^{(k)}$ is given by

$$\mathbf{r}_{\mathrm{dr,off}}^{(k)} = \mathbf{r}_{\mathrm{dr,off}}^{(k-1)} + \mathbf{K}_p' \cdot \Delta\mathbf{p}_{\mathrm{dr/pr}}^{(k-1)}\left(T^{(k-1)}\right) \tag{14}$$

where $\mathbf{K}_p' = \mathbf{diag}\left(k_{p_1}', k_{p_2}', k_{p_3}'\right)$ is a constant three-dimensional diagonal matrix with the diagonal elements $k_{p_1}', k_{p_2}', k_{p_3}' \in (0, 1)$.

The convergence of *Control Strategy 2* is given by the following theorem.

Theorem 2. *Consider the AAR system with the terminal positions of the drogue and the probe satisfying Eq. (3) and Eq. (4) respectively. Suppose the ILC controller is designed as Eq. (13), and its parameters satisfy*

$$0 < k_{p_i}' \le 1, \quad i = 1, 2, 3. \tag{15}$$

Then, through the repetitive docking attempts, the docking error $\Delta\mathbf{p}_{\mathrm{dr/pr}}^{(k)}\left(T^{(k)}\right)$ *will converge to a bound*

$$\lim_{k\to\infty} \left\| \Delta\mathbf{p}_{\mathrm{dr/pr}}^{(k)}\left(T^{(k)}\right) \right\| \le B_2$$

where

$$B_2 = \frac{2B_{\mathrm{pr}}}{\min\limits_{i=1,2,3}\left\{k_{p_i}'\right\}}.$$

Proof. See Appendix B. □

According to Theorem 2, the docking error $\Delta\mathbf{p}_{\mathrm{dr/pr}}^{(k)}\left(T^{(k)}\right)$ under the controller in Eq. (13) can converge to a bound. It is easy to verify that $B_2 < B_1$, where B_1 is the convergence bound of *Control Strategy 1* as defined in Eq. (11). This means the docking error of *Control Strategy 2* will be smaller than *Control Strategy 1*.

3.3. Control Strategy 3

Since *Control Strategy 1* is somewhat conservative and *Control Strategy 2* is somewhat aggressive, a compromised strategy is proposed in the form of piecewise function to combine their characteristics

$$\hat{\mathbf{r}}_{\mathrm{pr}}^{(k)}(t) = \begin{cases} \mathbf{r}_{\mathrm{dr,bow}}^{(k)}, & \Delta x_{\mathrm{dr/pr}}^{(k)}(t) > x_{\mathrm{a}} \\ \mathbf{p}_{\mathrm{dr}}^{(k)}(t) + \mathbf{r}_{\mathrm{dr,off}}^{(k)}, & 0 \le \Delta x_{\mathrm{dr/pr}}^{(k)}(t) \le x_{\mathrm{a}} \end{cases} \tag{16}$$

where $x_{\mathrm{a}} \in \mathbb{R}_+$ is the marginal distance determined by the strength distribution of the bow wave effect as shown in Fig. 5, which can be estimated by CFD analysis. For example, the x_{a} can be selected as the distance when the strength of the bow wave flow field reduces to 10% of its peak value, where $x_{\mathrm{a}} \approx 1$ m is recommended according to our CFD simulations. The idea is that the receiver first adopts *Control Strategy 1* to move to a fixed position close to the drogue, and then adopts *Control Strategy 2* in the final stage to decrease the docking error by introducing the position feedback.

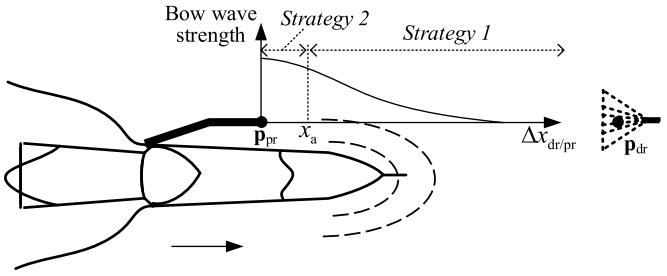

Fig. 5. Schematic diagram of *Control Strategy 3*.

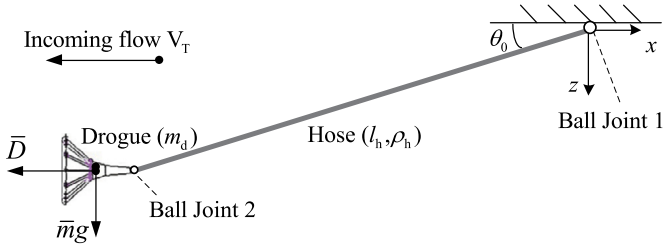

Fig. 6. Drogue dynamics pendulum model [27].

The convergence property of *Control Strategy 3* depends on the convergence properties of *Control Strategy 1* and *Control Strategy 2*. Therefore, the following conclusion is given without proof: if the parameters in Eq. (16) satisfy both Theorem 1 and Theorem 2, then *Control Strategy 3* can converge to a bound between B_1 and B_2.

3.4. Initial value estimator

This part proposes a simple method to estimate the drogue offset position based on the pendulum model as introduced in [27]. As shown in Fig. 6, the hose is treated as a rigid pendulum mounted to the tanker body and the drogue by two ball joints, and the pendulum is free to rotate around any axis. In Fig. 6, $\bar{m} \in \mathbb{R}_+$ denotes the equivalent total mass of the drogue and hose, $l_{\mathrm{h}} \in \mathbb{R}_+$ is the hose length, $\theta_0 \in \mathbb{R}_+$ is the pendulum angle to the oxy plane, and $\bar{D} \in \mathbb{R}_+$ denotes the equivalent drag on the drogue and hose. The equivalent mass $\bar{m}$ can be obtained through

$$\bar{m} = m_{\mathrm{d}} + \frac{1}{2}\rho_{\mathrm{h}} l_{\mathrm{h}} \tag{17}$$

where $m_{\mathrm{d}} \in \mathbb{R}_+$ is the drogue mass and $\rho_{\mathrm{h}} \in \mathbb{R}_+$ is the line density of the hose (defined as mass/length). Moreover, the equivalent drag force $\bar{D}$ can be obtained through moment equilibrium equation

$$\bar{D} = \frac{\bar{m}g\cos\theta_0}{\sin\theta_0}. \tag{18}$$

When a small disturbance force $\Delta\mathbf{F} \in \mathbb{R}^3$ is acting on the drogue, the drogue will move to a new equilibrium position with the position offset $\Delta\mathbf{p}_{\mathrm{dr}}$, where, according to Appendix C, the approximate relationship between $\Delta\mathbf{p}_{\mathrm{dr}}$ and $\Delta\mathbf{F}$ is

$$\Delta\mathbf{p}_{\mathrm{dr}} \approx \frac{l_{\mathrm{h}}}{\bar{m}g} \cdot \mathbf{R}_{\mathrm{L/F}} \cdot \Delta\mathbf{F} \tag{19}$$

where

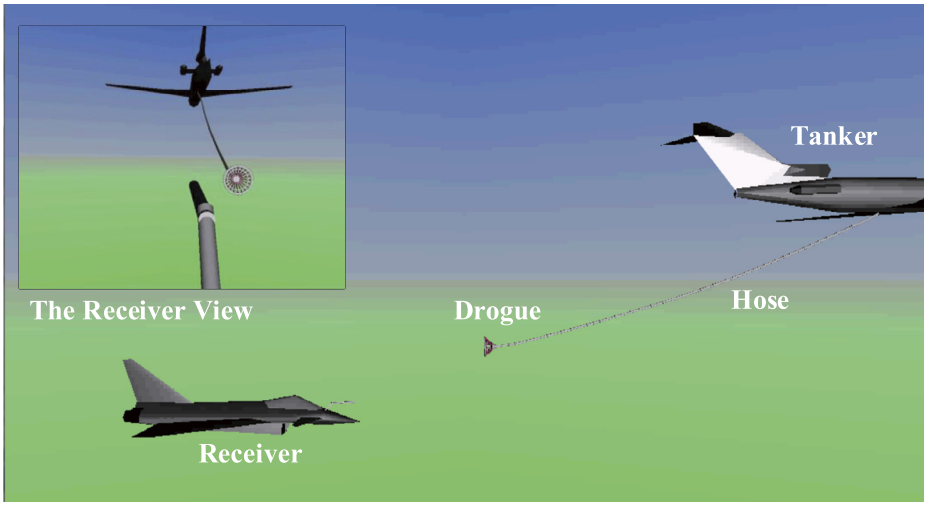

(a) 3D VR simulation environment

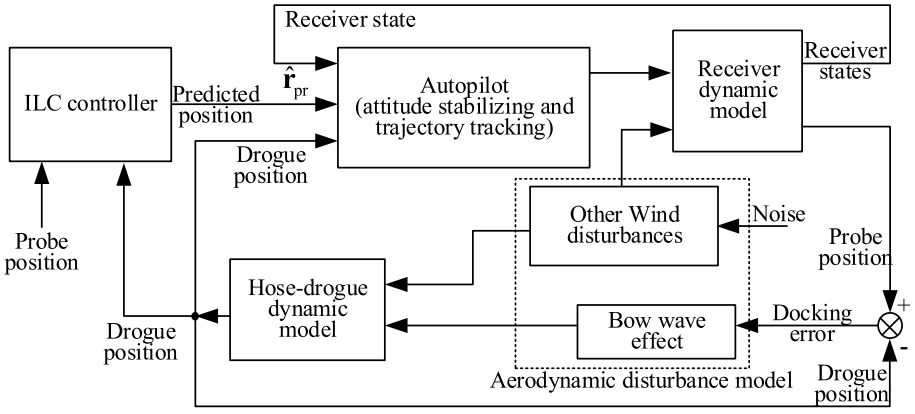

(b) Main structure of Simulink simulation environment

Fig. 7. MATLAB/SIMULINK based simulation environment for the AAR system.

$$\mathbf{R}_{L/F} \triangleq \begin{bmatrix} \sin^3\theta_0 & 0 & \sin^2\theta_0\cos\theta_0 \\ 0 & \sin\theta_0 & 0 \\ \sin^2\theta_0\cos\theta_0 & 0 & \sin\theta_0\cos^2\theta_0 \end{bmatrix}.$$

Since the drogue offset primarily comes from the bow wave effect, according to [21], the average force vector $\Delta\bar{\mathbf{F}}$ of the bow wave effect can be estimated by CFD-based system identification methods. Thus, by substituting $\Delta\bar{\mathbf{F}}$ into Eq. (19), the estimated position offset of the drogue $\Delta\mathbf{p}_{dr0}$ is given by

$$\Delta\mathbf{p}_{dr0} = \frac{l_h}{\bar{m}g} \cdot \mathbf{R}_{L/F} \cdot \Delta\bar{\mathbf{F}} \tag{20}$$

which can be used as the initial value for the drogue position offset estimation term $\mathbf{r}^{(k)}_{dr,bow}$ in Eq. (7) as

$$\mathbf{r}^{(0)}_{dr,bow} = \Delta\mathbf{p}_{dr0}. \tag{21}$$

The disturbance force $\Delta\bar{\mathbf{F}}$ is proportional to the dynamic pressure as

$$\Delta\bar{\mathbf{F}} \propto \frac{1}{2}\rho V_T^2 \tag{22}$$

where ρ is the air density determined by the altitude, and V_T is the flight speed. Thus, the learning result $\mathbf{r}_{dr,bow}$ in a specific refueling condition can be extended to any other refueling conditions through Eqs. (20)–(22).

4. Simulation and verification

4.1. Simulation configuration

A MATLAB/SIMULINK-based simulation environment with 3D virtual-reality display has been developed to simulate the docking stage of the AAR as shown in Fig. 7. Please refer to our previous work in [21,23] for the detailed information about the simulation environment.

The simulation parameters used in this paper are listed in Table 1, which includes the refueling conditions, the physical parameters of the drogue and the hose, and other parameters. The hose–drogue dynamics model used in this simulation is a 20-links-connected model according to [24,25]. The tanker is a KC-135 tanker, which is assumed to fly straight and level with constant speed. The receiver is an F-16 nonlinear model modified from the toolbox [28], which is a high fidelity model that can simulate the response of an actual F-16 by using the high-precision aircraft data. The bow wave effect model is obtained through the system identification method based on the CFD experimental data [20], and other wind effects, like the tanker vortex, the atmospheric turbulence, and the wind gust, are modeled according to [5] and specification MIL-F-8785C [29]. The autopilot of the AAR simulation system is an LQR-based controller according to [6,26], and the relative approaching speed along x-direction is constrained within 0.5 m/s–1 m/s according to NASA's report [1].

Table 1
Simulation configuration [21].

Parameter	Value
Refueling altitude h_T	3000 m
Refueling speed V_T	120 m/s
Air density ρ	0.909 kg/m^3
Drogue radius R_{dr}	0.35 m
Drogue coefficient C_d	0.81
Hose outside diameter D_h	33.6 mm
Hose density ρ_h (weight/length)	4.1 kg/m
Hose length l_h	15 m
Drogue mass m_d	39.5 kg m
Hose angle θ_0	20.5°
Criterion radius R_C	0.2 m

4.2. Controller implementation

In order to verify the effectiveness of the proposed ILC control methods, simulations are performed for the three docking strategies. The typical learning process of *Control Strategy 2* is presented in Fig. 8. There are three steps in each iteration of docking attempt: 1) the receiver remains at a standby position with a safe distance (about 5 m in the simulations) behind the drogue for several seconds (from 50 s to 60 s for the first docking attempt in Fig. 8) to observe the drogue movement and estimate the equilibrium position of the drogue; 2) the receiver approaches the drogue to perform a docking attempt (from 60 s to 71 s in Fig. 8) until the probe reaches the drogue center plane, where the success of fail of this docking attempt is judged; 3) The receiver returns to the standby postilion and gets ready for the next docking attempt.

There are four docking attempts presented in sequence (the start times are 50 s, 100 s, 150 s and 200 s respectively) in Fig. 8, where the first docking attempt fails, and the following three docking attempts all succeed. In the first docking attempt ($k = 1$) as shown in Fig. 8, the docking control ends at the terminal time $T^{(1)} = 71$ s, and this docking attempt is declared as failed because the radial error $\Delta R^{(1)}_{dr/pr} = 0.45$ m is larger than the desired radial error threshold $R_C = 0.2$ m. The subsequent docking attempts ($k > 4$) are not presented in Fig. 8, whose results are similar to attempt 4 with the radial errors floating within 0.06 m under the given turbulence intensity.

During the iterations, the offset values of the drogue are estimated by the ILC controller with the historical terminal positions. It is shown that the docking errors are decreased as the increase of the number of learning attempts, and finally converge into a bound which determines the success rate of the docking attempts.

4.3. Comparison of control strategies

By tuning the gains of the controller, the simulation environment can be adjusted to simulate receiver aircraft with different maneuverability. A series of simulations are performed to verify the proposed control strategies for receiver aircraft with different maneuverability. The docking curves of the successful docking attempts of the three control strategies are presented in Fig. 9. It can be observed from Fig. 9 that all the three strategies can achieve successful docking control after a few learning attempts, but their docking trajectories are different as shown in the dotted boxes. Under *Control Strategy 1*, the trajectories are smooth and steady despite the fast oscillation of the drogue due to disturbances. The reason is that this strategy is a pure feedforward control strategy, under which the probe always aims at a fixed position, and the drogue dynamics will never affect the probe movement. For low-maneuverability aircraft, the *Control Strategy 1* has the smoothest control signal which reduces the risk of the over control in the simulations. Therefore, *Control Strategy 1* is more suitable for low-maneuverability aircraft. Under *Control Strategy 2*, the receiver tracks the drogue all the time with a constant offset, so its trajectory oscillates along with the drogue and it has the minimum docking error. Simulations also indicate that *Control Strategy 2* is more suitable for high-maneuverability aircraft to reduce the docking error because the over control problem only occurs when the maneuverability is too slow. Under *Control Strategy 3*, the smoothness of the trajectories is between *Control Strategy 1* and *Control Strategy 2*. Therefore, the simulation results are consistent with the theoretical analysis.

According to our simulations, the success rate depends on many factors including the docking error threshold R_C and the strength

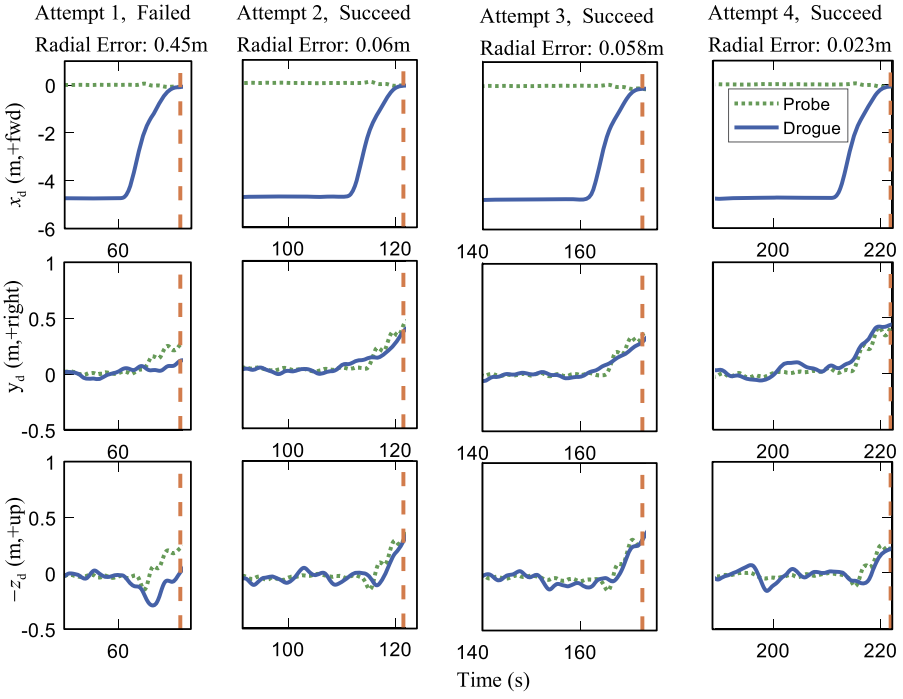

Fig. 8. Learning process with ILC *Control Strategy 2*.

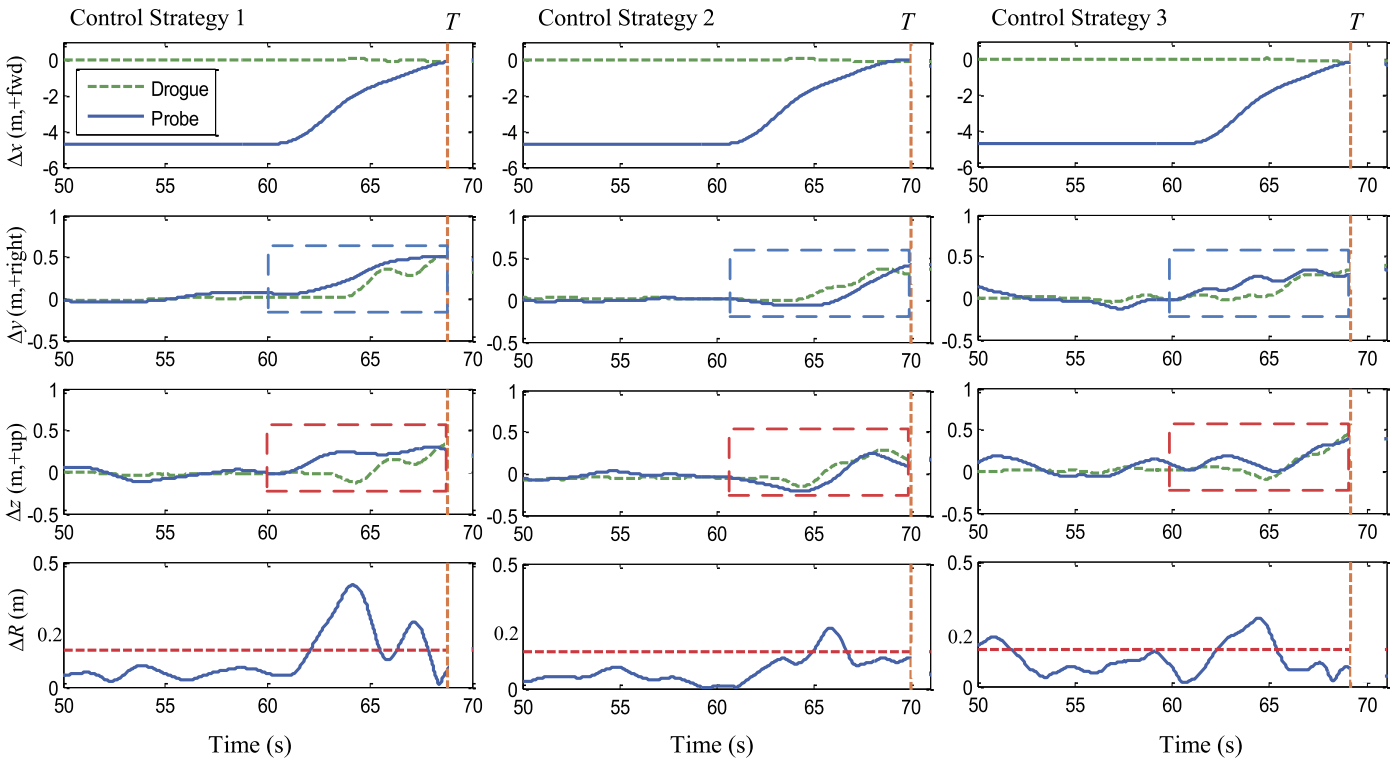

Fig. 9. Effects of the proposed three control strategies.

Table 2
Docking success rate under different atmospheric turbulence intensity.

Turbulence intensity	Small	Light	Moderate
Control Strategy 1	100%	43%	18%
Control Strategy 2	100%	74%	42%
Control Strategy 3	100%	52%	31%

Table 3
Drogue position offset under disturbance.

Condition	Offset	20-links	Pendulum
$F_z = 50$ N, $V_T = 150$ m/s	Δz	0.2543 m	0.249 m
$F_y = 50$ N, $V_T = 150$ m/s	Δy	0.2852 m	0.264 m
$F_z = 100$ N, $V_T = 150$ m/s	Δz	0.507 m	0.529 m
$F_z = 50$ N, $V_T = 200$ m/s	Δz	0.157 m	0.153 m
$F_z = 50$ N, $V_T = 120$ m/s	Δz	0.335 m	0.329 m

of the atmospheric turbulence. In these simulations, the tanker vortex disturbance comes from the model presented in [5], the wind gust and the atmospheric turbulence come from the MATLAB/SIMULINK Aerospace Blockset based on the mathematical representations from Military Specification MIL-F-8785C [29], and the bow wave effect disturbance comes from the authors' previous work [20]. The simulation results in Table 2 show that the proposed ILC control strategies are capable of achieving high-success docking control under the small turbulence intensity (stratosphere with good weather) and bow wave effect [5,21]. The "Small", "Light" and "Moderate" in Table 2 denote three different levels of turbulence intensities (probability of exceedance) for the atmospheric turbulence model defined in Military Specification MIL-F-8785C [29], where the moderate level of atmospheric turbulence has already been bad weather for precise docking control in the stratosphere. The docking success rate of each control strategy decreases from 100% to 0 as the turbulence intensity increases until it is even difficult for the receiver to maintain its position and attitude control. The results in Table 2 verify that the anti-disturbance capability sequence of the three control strategies is *Control Strategy 2* > *Control Strategy 3* > *Control Strategy 1*.

4.4. Effect of the initial value estimator

First, the simplified pendulum model is compared with the link-connected model in SIMULINK, where the link-connected model (with 20 links) is developed according to reference [30]. All the hose and drogue parameters are shown in Table 1. Some representative results calculated from Eq. (21) are compared with the results from the above mentioned link-connected model, and the comparison results are illustrated in Table 3. It is shown that the simplified pendulum model provides very similar results to the 20-rigid-link model, which illustrates the effectiveness of the proposed initial value estimation method.

Secondly, the average bow wave disturbance vector is selected as $\Delta\bar{\mathbf{F}} = [50\text{ N } 50\text{ N } -70\text{ N}]^{\mathrm{T}}$ according to the CFD simulations in [20,21]. By substituting $\Delta\bar{\mathbf{F}}$ into Eq. (20), the initial value for the learning controller can be obtained as $\mathbf{r}_{\mathrm{dr,bow}}^{(0)} = [-0.12\text{ m } 0.37\text{ m } -0.34\text{ m}]^{\mathrm{T}}$. The AAR simulations show that, with the estimated initial value and after enough number of learning attempts, the drogue offset will converge to $\mathbf{r}_{\mathrm{dr,bow}}^{(\infty)} \approx [-0.1\text{ m } 0.32\text{ m } -0.37\text{ m}]^{\mathrm{T}}$. It can be seen that the estimated initial value is close to the final one, which demonstrates that the proposed initial value estimation method is rather effective, and the learning speed can be improved significantly.

5. Conclusions

As analyzed in the paper, AAR is a dangerous task with the high precision requirement. The docking success rate is subject to the aircraft maneuverability and the strength of disturbances. This paper studies the PDR system model under various aerodynamic disturbances and proposes three ILC-based control methods to compensate for the errors caused by the aerodynamic disturbances. Since the receiver aircraft with low maneuverability requires larger

control signal to track the moving drogue which may cause the over control problem, the *Control Strategy 1* is more suitable for low-maneuverability aircraft because it tracks a fixed position in each iteration which may reduce the accuracy of the docking control. For receiver aircraft with high maneuverability, the *Control Strategy 2* is a better choice to improve the docking precision and anti-disturbance capability. For other receiver aircraft, the *Control Strategy 2* can provide a balance performance between safety and precision. Considering that ILC methods cannot completely compensate for the effect of the non-repetitive disturbances including atmospheric turbulence and wind gust, evaluation should be made according to the position fluctuation of the receiver and the drogue to determine whether the flight condition is suitable for a docking attempt. The proposed ILC initial value estimation method can predict the drogue position offset caused by disturbances and significantly improve the learning speed of the ILC methods. The simulation results demonstrate that the proposed control method is simple, efficient and robust for the docking control of AAR.

Conflict of interest statement

There is no conflict of interest.

Funding

This work was supported by the National Key Project of Research and Development Plan under Grant 2016YFC1402500 and the National Natural Science Foundation of China under Grant 61473012.

Appendix A. Proof of Theorem 1

According to [23], Eq. (3) can be further linearized around $\Delta\mathbf{p}_{\mathrm{dr/pr}}^{(k)}\left(T^{(k)}\right)=\mathbf{0}$ to simplify the convergence analysis of ILC, which yields

$$\mathbf{p}_{\mathrm{dr}}^{(k)}\left(T^{(k)}\right)\approx\mathbf{m}_0+\mathbf{M}_1\cdot\Delta\mathbf{p}_{\mathrm{dr/pr}}^{(k)}\left(T^{(k)}\right)+\mathbf{w}_{\mathrm{dr}}^{(k)} \tag{23}$$

where $\mathbf{M}_1\in\mathbb{R}^{3\times3}$ is a negative definite matrix (the bow wave effect decays as the distance increases along each direction), and $\mathbf{m}_0\in\mathbb{R}^3$ is a constant vector. Noteworthy, the linearization operation in Eq. (23) requires the variable $\Delta\mathbf{p}_{\mathrm{dr/pr}}^{(k)}\left(T^{(k)}\right)$ close to the linearized point $\mathbf{0}$, namely $\Delta\mathbf{p}_{\mathrm{dr/pr}}^{(k)}\left(T^{(k)}\right)\approx\mathbf{0}$. Therefore, if the terminal docking error is very large or tends to be very large (for example larger than 1 m) in one docking iteration due to the complex disturbance condition, then the docking process should be stopped immediately to avoid dangers or even casualties, and the data of this docking iteration should not be applied to the iterative learning controller.

First, the docking error at the kth docking attempt is defined according to Eq. (1) as

$$\Delta\mathbf{p}_{\mathrm{dr/pr}}^{(k)}\left(T^{(k)}\right)=\mathbf{p}_{\mathrm{dr}}^{(k)}\left(T^{(k)}\right)-\mathbf{p}_{\mathrm{pr}}^{(k)}\left(T^{(k)}\right). \tag{24}$$

Combining Eqs. (23), (24) gives

$$\mathbf{p}_{\mathrm{pr}}\left(T^{(k)}\right)=\mathbf{m}_0+(\mathbf{M}_1-\mathbf{I_3})\cdot\Delta\mathbf{p}_{\mathrm{dr/pr}}^{(k)}\left(T^{(k)}\right)+\mathbf{w}_{\mathrm{dr}}^{(k)}, \tag{25}$$

where $\mathbf{I}_3=\mathrm{diag}\,(1,1,1)$ is the three dimensional identity matrix. By substituting the ILC control (7) into the receiver model (4), one has

$$\mathbf{r}_{\mathrm{dr,bow}}^{(k)}-\mathbf{p}_{\mathrm{pr}}^{(k)}\left(T^{(k)}\right)=\mathbf{d}_{\mathrm{dr}}+\mathbf{w}_{\mathrm{pr}}^{(k)}. \tag{26}$$

Then, subtracting Eq. (26) with its $k-1$th expression gives

$$\mathbf{r}_{\mathrm{dr,bow}}^{(\mathbf{k})}-\mathbf{p}_{\mathrm{pr}}^{(\mathbf{k})}\left(\mathbf{T}^{(\mathbf{k})}\right)-\mathbf{r}_{\mathrm{dr,bow}}^{(k-1)}+p_{\mathrm{pr}}^{(k-1)}\left(T^{(k)}\right)=\mathbf{w}_{\mathrm{pr}}^{(k)}-\mathbf{w}_{\mathrm{pr}}^{(k-1)}. \tag{27}$$

Therefore, the $\mathbf{r}_{\mathrm{dr,bow}}^{(k)}$ and $\mathbf{p}_{\mathrm{pr}}^{(k)}\left(T^{(k)}\right)$ are eliminated by combining Eqs. (8), (25), (27), which yields

$$\Delta\mathbf{p}_{\mathrm{dr/pr}}^{(k)}\left(T^{(k)}\right)=\mathbf{A}\cdot\Delta\mathbf{p}_{\mathrm{dr/pr}}^{(k-1)}\left(T^{(k-1)}\right)+\mathbf{B}\cdot\tilde{\mathbf{w}}^{(k-1)} \tag{28}$$

where

$$\begin{aligned}\mathbf{A}&\triangleq\left(\mathbf{I_3}-\mathbf{M}_1+\mathbf{K}_p\right)^{-1}\left(\mathbf{I_3}-\mathbf{M}_1\right)\\ \mathbf{B}&\triangleq\left(\mathbf{I_3}-\mathbf{M}_1+\mathbf{K}_p\right)^{-1}\\ \tilde{\mathbf{w}}^{(k-1)}&\triangleq-\mathbf{v}_{\mathrm{pr}}^{(k)}+\mathbf{w}_{\mathrm{pr}}^{(k-1)}-\mathbf{w}_{\mathrm{dr}}^{(k)}+\mathbf{w}_{\mathrm{dr}}^{(k-1)}\end{aligned}.$$

Therefore, Eq. (28) can be written into the following form

$$\Delta\mathbf{p}_{\mathrm{dr/pr}}^{(k)}\left(T^{(k)}\right)=\mathbf{A}^k\cdot\Delta\mathbf{p}_{\mathrm{dr/pr}}^{(0)}\left(T^{(0)}\right)+\sum_{i=0}^{k-1}\mathbf{A}^i\mathbf{B}\cdot\tilde{\mathbf{w}}^{(k-i)}. \tag{29}$$

Since $\mathbf{M}_1$ and $\mathbf{K}_p$ are both diagonal matrices, it is easy to verify that the spectral radius of $\mathbf{A}$ is smaller than 1 ($\rho\,(\mathbf{A})<1$) when the constraints in Eq. (9) is satisfied, which yields

$$\rho\,(\mathbf{A})<1\Rightarrow\lim_{k\to\infty}\|\mathbf{A}\|^k=0. \tag{30}$$

Moreover, since the disturbances $\mathbf{w}_{\mathrm{pr}}^{(k)}$ and $\mathbf{w}_{\mathrm{dr}}^{(k)}$ are both bounded with $\left\|\mathbf{w}_{\mathrm{pr}}^{(k)}\right\|\le B_{\mathrm{pr}}$ and $\left\|\mathbf{w}_{\mathrm{dr}}^{(k)}\right\|\le B_{\mathrm{dr}}$, it is easy to obtain that $\tilde{\mathbf{w}}^{(k-1)}$ is also bounded with

$$\left\|\tilde{\mathbf{w}}^{(k-1)}\right\|\le2\sqrt{B_{\mathrm{pr}}^2+B_{\mathrm{dr}}^2}. \tag{31}$$

Then, the docking error $\Delta\mathbf{p}_{\mathrm{dr/pr}}^{(k)}\left(T^{(k)}\right)$ satisfies the following constraint

$$\begin{aligned}&\left\|\Delta\mathbf{p}_{\mathrm{dr/pr}}^{(k)}\left(T^{(k)}\right)\right\|\\ &\le\|\mathbf{A}\|^k\left\|\Delta\mathbf{p}_{\mathrm{dr/pr}}^{(0)}\left(T^{(0)}\right)\right\|+\sum_{i=0}^{k-1}\|\mathbf{A}\|^i\left\|\mathbf{B}\cdot\mathbf{v}^{(k-i)}\right\|\\ &\le\|\mathbf{A}\|^k\left\|\mathbf{X}^{(0)}\right\|+2\sqrt{B_{\mathrm{pr}}^2+B_{\mathrm{dr}}^2}\|B\|\sum_{i=0}^{k-1}\|\mathbf{A}\|^i\\ &=\|\mathbf{A}\|^k\left\|\mathbf{X}^{(0)}\right\|+2\sqrt{B_{\mathrm{pr}}^2+B_{\mathrm{dr}}^2}\|B\|\left(1-\|\mathbf{A}\|^k\right)\left(1-\|\mathbf{A}\|\right)^{-1}.\end{aligned} \tag{32}$$

Substituting Eq. (30) into Eq. (32) gives

$$\begin{aligned}\lim_{k\to\infty}\left\|\Delta\mathbf{p}_{\mathrm{dr/pr}}^{(k)}\left(T^{(k)}\right)\right\|&\le2\sqrt{B_{\mathrm{pr}}^2+B_{\mathrm{dr}}^2}\|B\|\left(1-\|\mathbf{A}\|\right)^{-1}\\ &\le\frac{2\sqrt{B_{\mathrm{pr}}^2+B_{\mathrm{dr}}^2}}{\min\limits_{i=1,2,3}\left\{k'_{p_i}\right\}}\triangleq B_1.\end{aligned} \tag{33}$$

Thus, the docking error $\Delta\mathbf{p}_{\mathrm{dr/pr}}^{(k)}\left(T^{(k)}\right)$ will converge to a bound B_1 as $k\to\infty$. In particular, by substituting $B_{\mathrm{dr}}=0$, $B_{\mathrm{pr}}=0$ into Eq. (33), one has $\lim_{k\to\infty}\left\|\Delta\mathbf{p}_{\mathrm{dr/pr}}^{(k)}\left(T^{(k)}\right)\right\|=0$.

Appendix B. Proof of Theorem 2

By letting $t=T^{(k)}$ in Eq. (13), the terminal value of *Control Strategy 2* is obtained as

$$\hat{\mathbf{r}}_{\mathrm{pr}}^{(k)}\left(T^{(k)}\right)=\mathbf{p}_{\mathrm{dr}}^{(k)}\left(T^{(k)}\right)+\mathbf{r}_{\mathrm{dr,off}}^{(k)}. \tag{34}$$

By combining Eq. (4) and Eq. (34), the term $\hat{\mathbf{r}}_{\mathrm{pr}}^{(k)}\left(T^{(k)}\right)$ is eliminated as

$$\begin{aligned}\mathbf{r}_{\mathrm{dr,off}}^{(k)} &= \mathbf{p}_{\mathrm{pr}}^{(k)}\left(T^{(k)}\right) - \mathbf{p}_{\mathrm{dr}}^{(k)}\left(T^{(k)}\right) + \mathbf{d}_{\mathrm{pr}} + \mathbf{w}_{\mathrm{pr}}^{(k)} \\ &= -\Delta\mathbf{p}_{\mathrm{dr/pr}}^{(k)}\left(T^{(k)}\right) + \mathbf{d}_{\mathrm{pr}} + \mathbf{w}_{\mathrm{pr}}^{(k)}. \end{aligned} \tag{35}$$

Then, substituting Eq. (35) into Eq. (14) gives

$$\Delta\mathbf{p}_{\mathrm{dr/pr}}^{(k)}\left(T^{(k)}\right) = \left(\mathbf{I} - \mathbf{K}_p'\right)\Delta\mathbf{p}_{\mathrm{dr/pr}}^{(k-1)}\left(T^{(k-1)}\right) + \tilde{\mathbf{v}}_{\mathrm{pr}}^{(k-1)}, \tag{36}$$

where $\tilde{\mathbf{v}}_{\mathrm{pr}}^{(k-1)} \triangleq \mathbf{w}_{\mathrm{pr}}^{(k)} - \mathbf{w}_{\mathrm{pr}}^{(k-1)}$ with bound $\left\|\tilde{\mathbf{v}}_{\mathrm{pr}}^{(k-1)}\right\| \le 2B_{\mathrm{pr}}$. Under the given condition $k_{p_1}', k_{p_2}', k_{p_3}' \in (0,1)$, there is $\rho\left(\mathbf{I} - \mathbf{K}_p'\right) < 1$, then

$$\left(\mathbf{I} - \mathbf{K}_p'\right)^k \to \mathbf{0}, \quad \text{as } k \to \infty.$$

Thus

$$\begin{aligned}&\lim_{k\to\infty}\left\|\Delta\mathbf{p}_{\mathrm{dr/pr}}^{(k)}\left(T^{(k)}\right)\right\| \\ &= \lim_{k\to\infty}\left\|\sum_{i=0}^{k-1}\left(\mathbf{I} - \mathbf{K}_p'\right)^i\tilde{\mathbf{v}}_{\mathrm{pr}}^{(k-i)}\right\| \\ &\le \lim_{k\to\infty}\sum_{i=0}^{k-1}\left\|\left(\mathbf{I} - \mathbf{K}_p'\right)\right\|^i\left\|\tilde{\mathbf{v}}_{\mathrm{pr}}^{(k-i)}\right\| \\ &\le \lim_{k\to\infty}\left(\sum_{i=0}^{k-1}\left\|\left(\mathbf{I} - \mathbf{K}_p'\right)\right\|^i\right)\cdot 2B_{\mathrm{pr}} = \frac{2B_{\mathrm{pr}}}{1 - \left\|\mathbf{I} - \mathbf{K}_p'\right\|} \\ &\le \frac{2B_{\mathrm{pr}}}{\min\limits_{i=1,2,3}\left\{k_{p_i}'\right\}} \triangleq B_2. \end{aligned}$$

In summary, the docking error $\Delta\mathbf{p}_{\mathrm{dr/pr}}^{(k)}\left(T^{(k)}\right)$ can converge to a bound B_2.

Appendix C. Pendulum model simplification

First, the drogue drag vector $\mathbf{D} \in \mathbb{R}^3$, the drogue gravity vector $\mathbf{G} \in \mathbb{R}^3$ and the equilibrium position of the drogue $\mathbf{L} \in \mathbb{R}^3$ are given in the tanker joint frame F_{T} as

$$\begin{aligned}\mathbf{D} &= \left[-\bar{D}\ \ 0\ \ 0\right]^{\mathrm{T}} \\ \mathbf{G} &= \left[0\ \ 0\ \ \bar{m}g\right]^{\mathrm{T}} \\ \mathbf{L} &= \left[-l_{\mathrm{h}}\cos\theta_0\ \ 0\ \ l_{\mathrm{h}}\sin\theta_0\right]^{\mathrm{T}}. \end{aligned} \tag{37}$$

When a small disturbance force $\Delta\mathbf{F} \triangleq \left[\Delta F_x\ \Delta F_y\ \Delta F_z\right]^{\mathrm{T}}$ is acting on the drogue, there will be a small position deviation of the drogue marked as $\Delta\mathbf{p}_{\mathrm{dr}} = \left[\Delta p_x\ \Delta p_y\ \Delta p_z\right]^{\mathrm{T}}$. Meanwhile, there will be a small angle deviation of the hose marked as $\Delta\theta$ and $\Delta\varphi$, where $\Delta\theta$ is the angle deviation on θ_0 as shown in Fig. 6, and $\Delta\varphi$ is the angle between the hose and the oxz plane. According to the projection relationship in Fig. 6, one has

$$\begin{aligned}\Delta p_x &= l_{\mathrm{h}}\cos\left(\Delta\varphi\right)\cos\left(\theta_0 + \Delta\theta\right) - l_{\mathrm{h}}\cos\left(\theta_0\right) \\ \Delta p_y &= l_{\mathrm{h}}\sin\left(\Delta\varphi\right) \\ \Delta p_z &= l_{\mathrm{h}}\cos\left(\Delta\varphi\right)\sin\left(\theta_0 + \Delta\theta\right) - l_{\mathrm{h}}\sin\left(\theta_0\right). \end{aligned} \tag{38}$$

Since $\Delta\theta$ and $\Delta\varphi$ are small values in practice, the following simplifications are made to simplify the expression

$$\sin\left(\Delta\theta\right) \approx \Delta\theta, \quad \cos\left(\Delta\varphi\right) \approx 1, \quad \sin\left(\Delta\varphi\right) \approx \Delta\varphi. \tag{39}$$

By substituting Eq. (39) into Eq. (38), one has

$$\Delta\mathbf{p}_{\mathrm{dr}} \approx l_{\mathrm{h}}\begin{bmatrix}\sin\left(\theta_0\right)\cdot\Delta\theta \\ \Delta\varphi \\ \cos\left(\theta_0\right)\cdot\Delta\theta\end{bmatrix}. \tag{40}$$

Meanwhile, according to the force moment equilibrium principle, there is

$$\mathbf{L} \times \left(\mathbf{D} + \mathbf{G}\right) = \mathbf{0} \tag{41}$$

$$\left(\mathbf{L} + \Delta\mathbf{p}_{\mathrm{dr}}\right) \times \left(\mathbf{D} + \mathbf{G} + \Delta\mathbf{F}\right) = \mathbf{0}, \tag{42}$$

where "$\times$" is the cross-product operation of vectors. With $\Delta\mathbf{p}_{\mathrm{dr}} \times \Delta\mathbf{F} \approx \mathbf{0}$, combining Eq. (41) and Eq. (42) yields that

$$\left(\mathbf{D} + \mathbf{G}\right) \times \Delta\mathbf{p}_{dr} \approx \mathbf{L} \times \Delta\mathbf{F}. \tag{43}$$

Solving Eq. (43) with Eqs. (37), (40) yields

$$\begin{aligned}\Delta\theta &\approx \frac{\sin^2\theta_0}{\bar{m}g}\Delta F_x + \frac{\cos\theta_0\sin\theta_0}{\bar{m}g}\Delta F_z \\ \Delta\varphi &\approx \frac{\sin\theta_0}{\bar{m}g}\Delta F_y. \end{aligned} \tag{44}$$

Then, combining Eq. (38) and Eq. (44) yields that

$$\Delta\mathbf{p}_{\mathrm{dr}} \approx \frac{l_{\mathrm{h}}}{\bar{m}g}\cdot\mathbf{R}_{\mathrm{L/F}}\cdot\Delta\mathbf{F} \tag{45}$$

where

$$\mathbf{R}_{\mathrm{L/F}} \triangleq \begin{bmatrix}\sin^3\theta_0 & 0 & \sin^2\theta_0\cos\theta_0 \\ 0 & \sin\theta_0 & 0 \\ \sin^2\theta_0\cos\theta_0 & 0 & \sin\theta_0\cos^2\theta_0\end{bmatrix}.$$

References

[1] R.P. Dibley, M.J. Allen, N. Nabaa, Autonomous airborne refueling demonstration phase I flight-test results, in: AIAA Atmospheric Flight Mechanics Conference and Exhibit, Aug. 2007, AIAA Paper 2007-6639.

[2] J.P. Nalepka, J.L. Hinchman, Automated aerial refueling: extending the effectiveness of unmanned air vehicles, in: AIAA Modeling and Simulation Technologies Conference and Exhibit, Aug. 2005, AIAA Paper 2005-6005.

[3] P.R. Thomas, U. Bhandari, S. Bullock, T.S. Richardson, J.L. Du Bois, Advances in air to air refuelling, Prog. Aerosp. Sci. 71 (2014) 14–35, https://doi.org/10.1016/j.paerosci.2014.07.001.

[4] K. Yue, L. Cheng, T. Zhang, J. Ji, D. Yu, Numerical simulation of the aerodynamic influence of an aircraft on the hose-refueling system during aerial refueling operations, Aerosp. Sci. Technol. 49 (2016) 34–40, https://doi.org/10.1016/j.ast.2015.11.011.

[5] A. Dogan, T.A. Lewis, W. Blake, Flight data analysis and simulation of wind effects during aerial refueling, J. Aircr. 45 (6) (2008) 2036–2048, https://doi.org/10.2514/1.36797.

[6] J.H. Lee, H.E. Sevil, A. Dogan, D. Hullender, Estimation of receiver aircraft states and wind vectors in aerial refueling, J. Guid. Control Dyn. 37 (1) (2013) 265–276, https://doi.org/10.2514/1.59783.

[7] A. Dogan, W. Blake, Modeling of bow wave effect in aerial refueling, in: AIAA Atmospheric Flight Mechanics Conference, Toronto, Canada, Aug. 2010, AIAA Paper 2010-7926.

[8] O. Khan, J. Masud, Trajectory analysis of basket engagement during aerial refueling, in: AIAA Atmospheric Flight Mechanics Conference, Jan. 2014, AIAA Paper 2014-0190.

[9] A. Dogan, S. Sato, W. Blake, Flight control and simulation for aerial refueling, in: AIAA Guidance, Navigation, and Control Conference and Exhibit, Aug. 2005, AIAA Paper 2005-6264.

[10] M.D. Tandale, R. Bowers, J. Valasek, Trajectory tracking controller for vision-based probe and drogue autonomous aerial refueling, J. Guid. Control Dyn. 29 (4) (2006) 846–857, https://doi.org/10.2514/1.19694.

[11] J. Wang, V.V. Patel, C. Cao, N. Hovakimyan, E. Lavretsky, Novel l1 adaptive control methodology for aerial refueling with guaranteed transient performance, J. Guid. Control Dyn. 31 (1) (2008) 182–193.

[12] J. Wang, N. Hovakimyan, C. Cao, L1 adaptive augmentation of gain-scheduled controller for racetrack maneuver in aerial refueling, in: AIAA Guidance, Navigation, and Control Conference, Aug. 2009, AIAA Paper 2009-5739.

[13] Z. Su, H. Wang, P. Yao, Y. Huang, Y. Qin, Back-stepping based anti-disturbance flight controller with preview methodology for autonomous aerial refueling, Aerosp. Sci. Technol. 61 (2017) 95–108, https://doi.org/10.1016/j.ast.2016.11.028.

[14] Q. He, H. Wang, Y. Chen, M. Xu, W. Jin, Command filtered backstepping sliding mode control for the hose whipping phenomenon in aerial refueling, Aerosp. Sci. Technol. 67 (2017) 495–505, https://doi.org/10.1016/j.ast.2017.04.020.

[15] J. Valasek, K. Gunnam, J. Kimmett, J.L. Junkins, D. Hughes, M.D. Tandale, Vision-based sensor and navigation system for autonomous air refueling, J. Guid. Control Dyn. 28 (5) (2005) 979–989, https://doi.org/10.2514/1.11934.

[16] M. Mammarella, G. Campa, M.R. Napolitano, M.L. Fravolini, Y. Gu, M.G. Perhinschi, Machine vision/GPS integration using EKF for the UAV aerial refueling problem, IEEE Trans. Syst. Man Cybern., Part C, Appl. Rev. 38 (6) (2008) 791–801.

[17] H. Zhu, S. Yuan, Q. Shen, Vision/GPS-based docking control for the UAV autonomous aerial refueling, in: 2016 IEEE Chinese Guidance, Navigation and Control Conference (CGNCC), IEEE, 2016, pp. 1211–1215.

[18] NATO, Atp-56(b) Air-To-Air Refuelling, Tech. rep., NATO, 2010.

[19] U. Bhandari, P.R. Thomas, S. Bullock, T.S. Richardson, J.L. du Bois, Bow wave effect in probe and drogue aerial refuelling, in: AIAA Guidance, Navigation, and Control Conference, Aug. 2013, AIAA Paper 2013-4695.

[20] Z.-B. Wei, X. Dai, Q. Quan, K.-Y. Cai, Drogue dynamic model under bow wave in probe-and-drogue refueling, IEEE Trans. Aerosp. Electron. Syst. 52 (4) (2016) 1728–1742, https://doi.org/10.1109/TAES.2016.140912.

[21] X. Dai, Z.-B. Wei, Q. Quan, Modeling and simulation of bow wave effect in probe and drogue aerial refueling, Chin. J. Aeronaut. 29 (2) (2016) 448–461, https://doi.org/10.1016/j.cja.2016.02.001.

[22] H.-S. Ahn, Y. Chen, K.L. Moore, Iterative learning control: brief survey and categorization, IEEE Trans. Syst. Man Cybern., Part C, Appl. Rev. 37 (6) (2007) 1099–1121, https://doi.org/10.1109/TSMCC.2007.905759.

[23] X. Dai, Q. Quan, J. Ren, Z. Xi, K.-Y. Cai, Terminal iterative learning control for autonomous aerial refueling under aerodynamic disturbances, J. Guid. Control Dyn. 41 (7) (2018) 1576–1583, https://doi.org/10.2514/1.G003217.

[24] K. Ro, J.W. Kamman, Modeling and simulation of hose-paradrogue aerial refueling systems, J. Guid. Control Dyn. 33 (1) (2010) 53–63, https://doi.org/10.2514/1.45482.

[25] Z.-B. Wei, Q. Quan, K.-Y. Cai, Research on relationship between drogue position and interference force for probe–drogue aerial refueling system based on link-connected model, in: 2012 31st Chinese Control Conference (CCC), IEEE, 2012, pp. 1777–1782 (in Chinese).

[26] B.L. Stevens, F.L. Lewis, Aircraft Control and Simulation, John Wiley & Sons, 2004.

[27] W.R. Williamson, E. Reed, G.J. Glenn, S.M. Stecko, J. Musgrave, J.M. Takacs, Controllable drogue for automated aerial refueling, J. Aircr. 47 (2) (2010) 515–527, https://doi.org/10.2514/1.44758.

[28] R.S. Russell, Non-Linear f-16 Simulation Using Simulink and Matlab, Tech. rep., University of Minnesota, 2003.

[29] D.J. Moorhouse, R.J. Woodcock, Background Information and User Guide For mil-f-8785c, Military Specification-Flying Qualities of Piloted Airplanes, Tech. Rep. AFWAL-TR-81-3109, U.S. Air Force Wright Aeronautical Labs, Wright–Patterson AFB, OH, July 1982.

[30] W. Ribbens, F. Saggio, R. Wierenga, M. Feldmann, Dynamic modeling of an aerial refueling hose & drogue system, in: 25th AIAA Applied Aerodynamics Conference, Jun. 2007, AIAA Paper 2007-3802.